Effect of Reactive Power Limit Modeling on Maximum System Loading and Active and Reactive Power Markets

Behnam Tamimi, *Student Member, IEEE,* Claudio A. Cañizares, *Fellow, IEEE,* and Sadegh Vaez-Zadeh, *Senior Member, IEEE*

***Abstract*—This paper presents a comparative investigation of various representations of reactive power limits in maximum loadability and active and reactive power market studies. Previously proposed optimal power flow (OPF) models for these types of analyses are first reviewed and briefly discussed. Different models for representing reactive power limits in these optimization problems are then presented, concentrating in particular on the proper modeling of the generators' capability curves as terminal voltages change, which has been identified as a shortcoming of previous studies. Comparative numerical analyses of the effect of various reactive power limit models in maximum loading and active and reactive power dispatch and pricing levels are presented and discussed, to thus quantify the effect these various limit representations have on the corresponding results. Two test systems, namely, the CIGRE-32 benchmark system and a 1211-bus dispatch model of a European network, are used for numerical studies. The presented results show that in most OPF applications, the improvement on the reactive power limits representation lead to subtle differences at the cost of increased computational complexity, which in some cases may be difficult to justify in practice.**

***Index Terms*—Reactive power limits, generator capability curves, maximum loadability, voltage stability, electrical energy markets, reactive power markets, optimal power flows.**

I. Introduction

SYNCHRONOUS generators are a primary source of reactive power in electric power systems. Although there are other important reactive power sources such as shunt capacitors and Flexible AC Transmission System (FACTS) controllers (e.g. Static Var Compensators or SVCs and Shunt Static Synchronous Compensator or STATCOMs), to a great extent, generators are responsible for maintaining adequate voltage profiles across the systems [1]. Consequently, their characteristics and their limitations are of major importance for the analysis of power grids, particularly when the system is operated near its limits. This is even more relevant under the current competitive market environment, as economic pressures from market participants force the grid to supply the required demand with widely varying suppliers while still guaranteeing the operational and security limits of the system [2]. Therefore, the economic performance of electricity markets is directly related to the level which the systems', and especially generators', capabilities are fully recognized and deployed.

The stability and security limits of power systems can be closely approximated by voltage stability criteria [3]. In almost all voltage instability incidents, one or more synchronous generators reached its reactive power limits (Q-limits) [1]; thus, the proper modeling of the reactive power capabilities of generators is of crucial importance for voltage stability studies. Various models have been proposed for the representation of Q-limits of synchronous generators in voltage stability and market analyses. Therefore, this paper starts with comparing the results of using these models in the aforementioned studies, to highlight their shortcomings and advantages.

There are two dominant approaches to voltage stability studies, namely, Continuation Power Flow (CPF) and, more recently, Optimal Power Flow (OPF) based approaches; the latter are also referred to as OPF-Direct Methods (OPF-DM) [3]. In the CPF method, the loading level is increased until there is no feasible solution to the power flow equations or the solution does not satisfy required ranges for certain system variables such as voltages or power transfers [4]. The OPF-DM, on the other hand, is mainly an optimization problem that maximizes the system loadability while satisfying operational constraints, including the power flow equations as well as limits on generator reactive powers, voltages and power transfers, as discussed for example in [5], [6]. Depending on the way the generator voltage control is modeled, the results obtained from an OPF-DM can be shown to be basically the same as those obtained from the CPF method [7]. In most of these studies, generators' Q-limits have been usually modeled as simple fixed limits to reduced computational burden and avoid convergence problems, in spite of the key role that these limits play in voltage instability phenomenon, as discussed for example in [2] and [8]. In the latter two papers, the generator capability curves are better represented in voltage stability studies, modeling the voltage dependence of generator Q-limits.

A variety of OPF models are widely used to dispatch generators and obtain pricing signals in electrical energy markets [9]–[12]. More sophisticated market OPF models have

Manuscript submitted December 2008; revised and resubmitted May 2009; accepted June 2009.

This work was partially supported by grants from CFI, NSERC and MITACS, Canada. This work was also partially supported by the University of Tehran through the research grant of the third author.

B. Tamimi and S. Vaez-Zadeh are with the Department of Electrical and Computer Engineering, University of Tehran, Iran (e-mail: btamimi@ieee.org).

C. A. Cañizares is with the Department of Electrical and Computer Engineering, University of Waterloo, Waterloo, ON, N2L-3G1, Canada (e-mail: ccanizar@uwaterloo.ca).

been also proposed, where, for example, voltage stability and market clearance problems are jointly considered in the OPF formulation [6], [13], [14]. In the majority of these market auction models, generators Q-limits are assumed as fixed values.

OPF-based approaches have been also proposed to efficiently formulate a reactive power market problem, provided that generators capability curves are properly modeled and deployed [15], [16]. In [17], a better representation of Q-limits in electricity markets is discussed, proposing as well an OPF-based formulation for reactive power contracting. The authors in [18] propose a reactive power market structure in which the reactive power management and pricing problem is divided into two stages, namely, a seasonal procurement process and a real-time dispatch problem; in this paper, an OPF-based procedure for optimal procurement and pricing of reactive power is also proposed and discussed. In both [17] and [18], the effect of generated active power on the associated Q-limits is explicitly modeled; however, it is assumed that these limits are independent of the terminal voltage magnitude. Finally, the authors in [19] and [20] use an OPF model to represent generator Q-limits in a mixed active and reactive power market real-time auction, implicitly accounting for rotor and stator current limits in the modeling. However, no discussions or comparisons on the effect of this modeling in the market output variables is presented; moreover, the proposed OPF formulation presents various pitfalls as discussed in [18].

Based on the literature review, the present paper concentrates on comprehensibly addressing some of the shortcomings observed in previous publications. Therefore, different models of generator Q-limits are discussed in detail, comparing their effect on system loadability as well as electricity market OPF-models for both active and reactive powers. Three OPF-based models for the study of maximum system loadability and market studies, considering the precise and practical representation of generator Q-limits, are presented, discussed and compared based on the results obtained for two realistic test systems. The estimation of missing data required for the proposed models is also discussed. Improvements to a previously proposed solution technique for the Mixed Integer Nonlinear Programming (MINLP) problem associated with the reactive power procurement OPF model are presented as well.

The paper is organized as follows: In Section II, a brief background review of previously proposed OPF models and the representation of generator Q-limits in voltage stability, active power market auctions, and reactive power procurement is presented. Section III discusses the proposed OPF models that properly represent the generator capability curves through explicit limits on rotor and stator currents; this section also presents improvements to the solution technique of the Q-procurement MINLP OPF problem. A detailed comparative analysis of the effect of various Q-limit representations on system loadability and active and reactive powers market studies is presented in Section IV; the 32-bus CIGRE test system and a 1211-bus model of a European network are used in these analyses. Finally, Section V summarizes the main results and contributions of the present paper.

II. Background

A. OPF-DM Formulation

As discussed in the previous section, OPF models have been proposed for maximum loadability calculations in voltage stability studies. An OPF model with complementarity constraints is proposed in [6], [7], where it is shown that it yields the same maximum loadability results as a CPF technique. In this formulation, the generator voltage controls are modeled explicitly; thus, when the generator's reactive power limits are reached, the machine loses control over its terminal voltage. The latter is mathematically represented in this model using complementarity constraints, which for a generator k can be written as follows:

$$0 \leq (Q_{Gk} - Q_{Gk\,\min}) \perp V_{ak} \geq 0 \;\Rightarrow\; (Q_{Gk} - Q_{Gk\,\min})\, V_{ak} = 0 \tag{1a}$$

$$0 \leq (Q_{Gk\,\max} - Q_{Gk}) \perp V_{bk} \geq 0 \;\Rightarrow\; (Q_{Gk\,\max} - Q_{Gk})\, V_{bk} = 0 \tag{1b}$$

$$V_{tk} = V_{tko} + V_{ak} - V_{bk} \tag{1c}$$

where V_t represents the generator terminal voltage magnitude; Q_G stands for the generator reactive power output; $\perp$ stands for the *complement* operator; V_a and V_b are auxiliary, nonnegative variables that allow increasing or decreasing the generator terminal voltage, depending on the value of Q_G; and V_{tko} is the k^{th} generator terminal voltage set-point.

B. OPF Market Auction Model

An optimal set of electric power transactions can be calculated by using a proper OPF formulation. Usually the objective of this optimization problem is the minimization of electricity production costs or the maximization of social benefit or social welfare [10], [11]. Nodal electricity prices or Locational Marginal Prices (LMPs) are a byproduct of the OPF solution at no extra computational cost. Moreover, the inclusion of system operational and security constraints in an OPF model is straight-forward. It should be noted that, in this OPF model, there is no need for complementarity constraints as in the previous subsection, since the aim here is to obtain the "optimal" generator terminal voltage set-points, which are bounded above and below.

C. Reactive Power Procurement Problem

An optimal set of generators for providing reactive power in the grid can be determined on a seasonal basis by an appropriate OPF formulation [17], [18]. Due to the local nature of reactive power, this problem should be implemented for different voltage zones. Note that it is not proposed as a mechanism for real-time reactive power dispatch. The procurement procedure is assumed to be based on generators being compensated for availability, energy losses, and opportunity costs associated with active power output reductions due to the required reactive power provision and generator capability limits. The assumed structure of reactive power offers from generators is depicted in Fig.1.

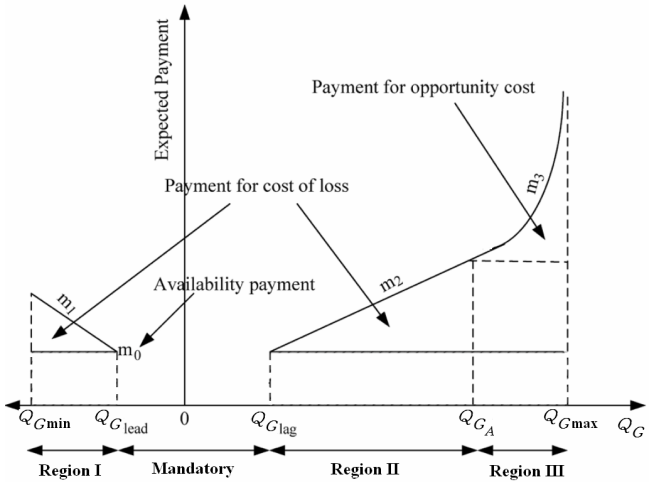

Fig. 1. Reactive power offers from generators and the three operating regions.

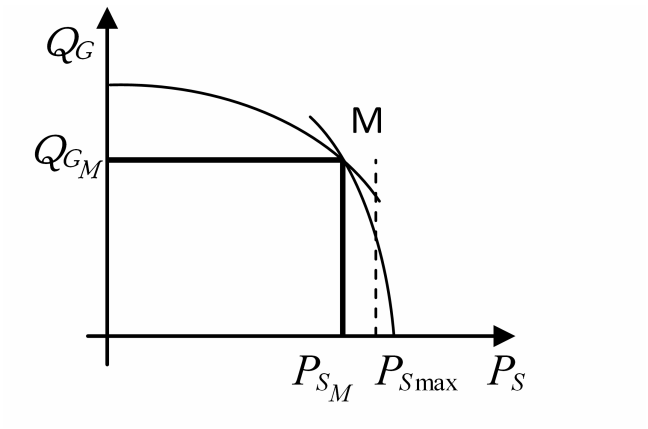

Fig. 2. Representation of reactive power maximum limits.

The objective function of the procurement OPF problem is a "societal advantage function" (SAF), which is defined as the aggregate system benefits gained from reactive power services minus the expected payments by the system operator. The SAF for a given zone k is expressed as follows [18]:

$$\begin{aligned} SAF_k = &-\rho_{0_k} - \sum_{i\in k} x_{1_i}\left(C_L\left|\mu_i\right| - \rho_{1_k}\right)\left(Q_{G1_i} - Q_{G_{\text{lead}}}\right) \\ &+ \sum_{i\in k} x_{2_i}\left(C_L\left|\eta_i\right| - \rho_{2_k}\right)\left(Q_{G2_i} - Q_{G_{\text{lag}}}\right) \\ &+ \sum_{i\in k} x_{3_i}\left(C_L\left|\gamma_i\right| - \rho_{2_k}\right)\left(Q_{G3_i} - Q_{G_{\text{lag}}}\right) \\ &- 0.5\rho_{3_k} x_{3_i}\left(Q_{G3_i} - Q_{G_{Ai}}\right)^2. \end{aligned} \quad (2)$$

Here, Q_{G1_i}, Q_{Gd_i}, Q_{G2_i}, and Q_{G3_i} are reactive power variables representing the 4 regions for the i^{th} generator, i.e. under-excitation, mandatory, over-excitation and opportunity regions, respectively, as per Fig.1, where the parameters $Q_{G_{\text{lag}}}$, $Q_{G_{\text{lead}}}$ and Q_{G_A} are defined. The variables x_{1_i}, x_{d_i}, x_{2_i} and x_{3_i} are binary variables associated with the aforementioned 4 reactive power generating regions, to model the generator operation in only one of these regions at a time. The parameters μ, η and γ are sensitivity factors of the system's maximum loadability with respect to $Q_{G\min}$, $Q_{G\max}$ and Q_G, respectively, obtained from the OPF-DM problem; these parameters are meant to represent the marginal benefit of generator's reactive powers with respect to system security. The parameter C_L is a loadability cost parameter ($/MWh) representing the monetary value of system security. The variables ρ_1 ($/Mvar) and ρ_2 ($/Mvar) are the zonal prices for energy losses in the under and over-excitation regions, and ρ_3 ($/Mvar/Mvar) and ρ_0 ($/Mvar) are the zonal uniform opportunity and availability price components, respectively.

The reactive power procurement OPF problem is formulated in [17], [18] based on the zonal objective function (2) and system operational constraints. Given the presence of integer variables, this is an MINLP problem, i.e. it is discontinuous and nonconvex, and hence there is a need for special solvers and/or solution techniques to obtain a solution. Thus, a heuristic iterative approach to transform this MINLP problem into a series of Non-linear Programming (NLP) problems is proposed and discussed in [18]. An improved solution approach based on sensitivities of SAF with respect to the different regions of generator reactive power operation is proposed in Section III.

It should be mentioned that the reactive power market structures and associated models existent in the literature concentrate mainly on generators. Appropriate market mechanisms for managing and pricing other reactive power sources such as SVC and STATCOM FACTS controllers have yet to be proposed and discussed.

D. Representation of Q-limits

Economical usage of power system capabilities is critical due to the scarcity of resources and increasing demand. Hence, it has been proposed to model generator reactive power maximum limits as a function of its active power output to better employ its capabilities [17], [18]. The model is depicted graphically in Fig.2 for a given terminal voltage V_{to}, where the intersection of the maximum field (rotor) induced voltages $E_{f\max}$ and the maximum stator current $I_{a\max}$ is noted as a point M. It can be reasonably assumed that P_{S_M} typically represents the rated active power, which is typically close to the maximum active power output $P_{S\max}$, and Q_{G_M} stands for the maximum reactive power usually stated in the power flow data set. The maximum reactive power limit in this case can be stated mathematically as follows:

$$Q_{G1\max} = \sqrt{\left(\frac{V_{to}\ E_{f\max}}{X_S}\right)^2 - P_S^2} - \frac{V_{to}^2}{X_S} \quad (3a)$$

$$Q_{G2\max} = \sqrt{\left(V_{to}\ I_{a\max}\right)^2 - P_S^2} \quad (3b)$$

$$Q_{G\max} = \begin{cases} Q_{G1\max} & \text{if } P_S < P_{S_M} \\ Q_{G2\max} & \text{if } P_S > P_{S_M} \end{cases} \quad (3c)$$

where P_S is the generator active power output; $Q_{G1\max}$ and $Q_{G2\max}$ represent reactive power limits due to maximum field

and stator currents, respectively; and X_S is the machine's synchronous reactance. This reactive power limit representation can be readily added to the OPF-DM model and the OPF auction model, as proposed in [17], [18].

Observe in (3) that there is a switching behavior in the maximum reactive power limit depending on the value of generated active power. Because of this discontinuity, this model can lead to computational problems during the OPF solution process, especially in the presence of complementarity constraints. In fact, due to these convergence issues, the generators' active power outputs were assumed constant in the OPF models discussed in [17], [18]. Since the generator terminal voltage magnitude is unknown in the OPF model, choosing a priori fixed value for this variable to model the generator capability curves is an approximation that may lead to errors in the final results, as discussed in Section IV. The models proposed and discussed in Section III and tested in Section IV demonstrate that this assumption is not really necessary.

The reason for the aforementioned errors can be clearly shown by the following analysis: If the partial derivatives of $Q_{G1\max}$ and $Q_{G2\max}$ with respect to V_t are calculated, for typical values of variables and parameters, one has, as per Fig.3, that:

$$\left.\frac{\partial Q_{G1\max}}{\partial V_t}\right|_{V_{to}} \approx 0^- \tag{4a}$$

$$\left.\frac{\partial Q_{G2\max}}{\partial V_t}\right|_{V_{to}} \geq 0 \tag{4b}$$

This means that, if for example, the actual voltage value of the OPF solution is smaller than the chosen V_{to} value, then $Q_{G1\max}$ is slight smaller than the actual Q-limit associated with the maximum rotor current. On the other hand, $Q_{G2\max}$ would be larger than the actual limit associated with the maximum stator current.

III. Proposed OPF Models

Equations (3a) and (3b) can be simply rewritten as follows, for any value of V_t, E_f and I_a:

$$\left(Q_G + \frac{V_t^2}{X_S}\right)^2 + P_S^2 - \left(\frac{V_t\, E_f}{X_S}\right)^2 = 0. \tag{5}$$

$$P_S^2 + Q_G^2 = (V_t\ I_a)^2 \tag{6}$$

The effect of limits on E_f and I_a as the terminal voltage V_t changes can be considered explicitly in these equations, leading to the capability polyhedron illustrated in Fig.3 [21], instead of the typical 2D capability charts. Note that as the terminal voltage increases, the capability limits associated with I_a increase significantly, whereas those associated with E_f decrease very slightly (for all practical purposes these can be assumed to remain unchanged).

Pole saliency affects only (5). In [8], it is argued that this cylindrical rotor equation is more conservative, guaranteeing the preservation of limits in the salient pole case. Hence, this equation can be used as an approximation for the salient pole case to represent the effect of maximum allowable rotor current on the generator's capability.

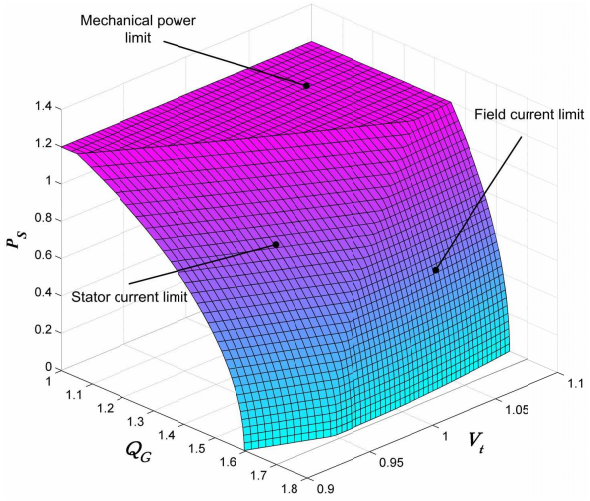

Fig. 3. The polyhedron of voltage-dependent reactive power limits obtained by the p.u. parameter values with respect to the system base values as: $E_{f\max} = 1.903$, $I_{a\max} = 1.772$, $X_S = 0.538$

Equations (5) and (6), together with upper limits on E_f and I_a, can be readily included in the OPF-DM, OPF market auction and reactive power procurement formulations to better represent the generators' capability curves. Note that there are no discontinuities in these equations. It should be mentioned that the lower limits in generated reactive power should be still represented through fixed values, since this models better the generator behavior in the under-excitation region [17].

A. Maximum Loading OPF Model

Using (5) and (6) to represent the generator capabilities in the OPF-DM model leads to the following improved optimization model:

$$\max \quad \lambda \tag{7a}$$

$$\text{s.t.} \quad G(\delta, V_L, K_G, V_t, Q_G, P_S, P_D, Q_D, E_f, I_a, \lambda) = 0 \tag{7b}$$

$$P_S \leq P_{S\max} \tag{7c}$$

$$\left(Q_G + \frac{V_t^2}{X_S}\right)^2 + P_S^2 - \left(\frac{V_t\, E_f}{X_S}\right)^2 = 0 \tag{7d}$$

$$P_S^2 + Q_G^2 = (V_t\ I_a)^2 \tag{7e}$$

$$0 \leq \begin{pmatrix} Q_G - Q_{G\min} \\ E_{f\max} - E_f \\ I_{a\max} - I_a \end{pmatrix} \perp \begin{pmatrix} V_a \\ V_b \\ V_c \end{pmatrix} \geq 0 \tag{7f}$$

$$V_t = V_{to} + V_a - V_b - V_c \tag{7g}$$

$$V_{L\min} \leq V_L \leq V_{L\max} \tag{7h}$$

Here, the vector function G represents the power flow equations; δ stands for the bus-voltage phase angles; V_L is the set of load voltage magnitudes; and P_D and Q_D stand for the loads' active and reactive powers, respectively. The variable λ is the loading factor, and K_G is a scalar value used to model a distributed slack bus; these variables basically define the

generator output and load levels as follows:

$$P_S = (1 + \lambda + K_G)P_{Go} \tag{8a}$$
$$P_D = (1 + \lambda)P_{Lo} \tag{8b}$$
$$Q_D = (1 + \lambda)Q_{Lo} \tag{8c}$$

where P_{Go}, P_{Lo} and Q_{Lo} are generation active powers and load active and reactive powers base values.

The loss of voltage control due to stator and rotor current limits is modeled by the complementarity constraints (7f). Observe that, according to [22], the larger number of complementarity constraints may increase the non-smoothness of the loadability surface in comparison to the model with simple fixed Q-limits, given the larger number of generator possible states.

B. OPF Market Model

The OPF market model can also be improved by replacing the fixed reactive power limits with the proposed generator capability model, resulting in the following model:

$$\max \quad SB = \sum_{j\in\mathcal{D}} C_{Dj}P_{Dj} - \sum_{i\in\mathcal{G}} C_{Si}P_{Si} \tag{9a}$$
$$\text{s.t.} \quad G(\delta, V_L, V_t, Q_G, P_S, P_D, E_f, I_a) = 0 \tag{9b}$$
$$P_{S\min} \le P_S \le P_{S\max} \tag{9c}$$
$$P_{D\min} \le P_D \le P_{D\max} \tag{9d}$$
$$\left(Q_G + \frac{V_t^2}{X_S}\right)^2 + P_S^2 - \left(\frac{V_t\, E_f}{X_S}\right)^2 = 0 \tag{9e}$$
$$P_S^2 + Q_G^2 = (V_t\ I_a)^2 \tag{9f}$$
$$0 \le E_f \le E_{f\max} \tag{9g}$$
$$0 \le I_a \le I_{a\max} \tag{9h}$$
$$Q_{G\min} \le Q_G \tag{9i}$$
$$V_{t\min} \le V_t \le V_{t\max} \tag{9j}$$
$$V_{L\min} \le V_L \le V_{L\max} \tag{9k}$$
$$P_{ij}(\delta, V_L, V_t) \le P_{ij\max} \qquad \forall (i,j) \in \mathcal{T} \tag{9l}$$

where the SB objective function stands for the social benefit (social welfare); $\mathcal{D}$ and $\mathcal{G}$ represent the set of loads and generators, respectively; and C_D and C_S stand for the corresponding demand and supply bids. The variable P_{ij} represents the power flow over a transmission component (i,j), which is bounded due to operational/security limits, and $\mathcal{T}$ is the set of transmission components. The demand's power factor is typically assumed constant, thus the corresponding reactive power is not a variable, being proportional to its active power. In the case of inelastic demand, P_D is fixed and $C_D = 0$, resulting in SB solely representing generated power costs for the system.

C. Reactive Power Procurement Model

The procurement model can also be improved as the previous OPF-models by replacing the fixed reactive power upper limits with the proposed generator capability representation, resulting in the following model:

$$\max \quad SAF = \sum_k SAF_k \tag{10a}$$
$$\text{s.t.} \quad G(\delta, V_L, V_t, Q_G, E_f, I_a) = 0 \tag{10b}$$
$$\left(Q_G + \frac{V_t^2}{X_S}\right)^2 + P_S^2 - \left(\frac{V_t\, E_f}{X_S}\right)^2 = 0 \tag{10c}$$
$$P_S^2 + Q_G^2 = (V_t\ I_a)^2 \tag{10d}$$
$$0 \le E_f \le E_{f\max} \tag{10e}$$
$$0 \le I_a \le I_{a\max} \tag{10f}$$
$$x_1 Q_{G\min} \le Q_{G1} \le x_1 Q_{G_{\text{lead}}} \quad : \overline{\alpha_1} \tag{10g}$$
$$\underline{\alpha_d} : x_d Q_{G_{\text{lead}}} \le Q_{Gd} \le x_d Q_{G_{\text{lag}}} \quad : \overline{\alpha_d} \tag{10h}$$
$$\underline{\alpha_2} : x_2 Q_{G_{\text{lag}}} \le Q_{G2} \le x_2 Q_{G_A} \quad : \overline{\alpha_2} \tag{10i}$$
$$\underline{\alpha_3} : x_3 Q_{G_A} \le Q_{G3} \tag{10j}$$
$$x_1 + x_d + x_2 + x_3 = 1 \tag{10k}$$
$$Q_G = Q_{G1} + Q_{Gd} + Q_{G2} + Q_{G3} \tag{10l}$$
$$V_{t\min} \le V_t \le V_{t\max} \tag{10m}$$
$$V_{L\min} \le V_L \le V_{L\max} \tag{10n}$$
$$P_{ij}(\delta, V_L, V_t) \le P_{ij\max} \qquad \forall (i,j) \in \mathcal{T} \tag{10o}$$
$$(1 - x_d)m_{0_i} \le \rho_{0_k} \quad \text{if } Q_{G_i} \ne 0, \quad \forall i \in k, \forall k \tag{10p}$$
$$x_{1_i} m_{1_i} \le \rho_{1_k} \quad \forall i \in k, \forall k \tag{10q}$$
$$x_{2_i} m_{2_i} \le \rho_{2_k} \quad \forall i \in k, \forall k \tag{10r}$$
$$x_{3_i} m_{3_i} \le \rho_{3_k} \quad \forall i \in k, \forall k \tag{10s}$$

where m_{0_i}, m_{1_i}, m_{2_i} and m_{3_i} are the i^{th} generator bid offers, as defined in Fig.1, and x_d is a binary variable associated with the *Mandatory* region depicted in this figure. The zonal pricing is modeled by (10p)-(10s). Note that (10k) guarantees that only one of four Regions I, II, III or Mandatory illustrated in Fig.1 would be active at any given time. Observe that even though Q_A may change with V_t, depending on the active power dispatch level of the generator, from the discussions in Section II.D with respect to Fig.2, generators will likely be dispatched at nominal power (P_{SM}), and hence, based on (4a), the value of Q_A will not change considerably with the generator's terminal voltage; this assumption significantly simplifies the model for computational purposes. Equations (10g)-(10j) are constraints representing the various reactive power generating regions, and the $Q_{G\max}$ limit has been replaced by explicit limits on E_f and I_a. The variables $\overline{\alpha_1}$, $\underline{\alpha_d}$, $\overline{\alpha_d}$, $\underline{\alpha_2}$, $\overline{\alpha_2}$ and $\underline{\alpha_3}$ stand for the Lagrange multipliers associated with the corresponding constraints. These variables represent the sensitivity of SAF with respect to the associated limits; for instance, $\overline{\alpha_2}$ yields the sensitivity of SAF with respect to Q_G as it "moves" from Region II into Region III. These sensitivity factors are used to turn this MINLP problem into a series of NLP problems, as explained next.

A somewhat similar iterative approach to the one described in [18] is used here to solve the MINLP problem (10). The proposed iterative approach is illustrated in Fig.4 and Fig.5, and starts by fixing the binary variables x based on an initial feasible point, which transforms (10) into an NLP problem that can be solved using "standard" solvers. At the end of each iteration, the binary variables are changed according

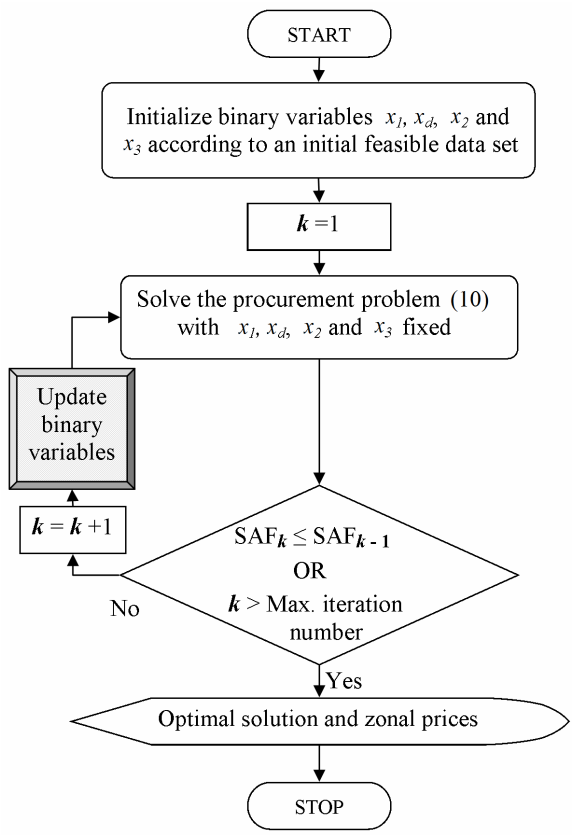

Fig. 4. Proposed MINLP solution procedure.

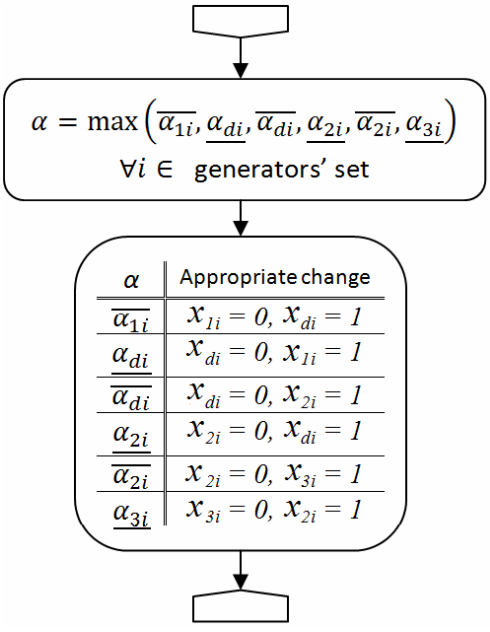

Fig. 5. Binary variables update procedure in Fig.4.

to the aforementioned α sensitivity factors, which basically indicate which generators and associated limits improve the SAF objective function the most; according to these values, the corresponding binary variables are modified as per Fig.5, one generator at the time. The iterative process stops when SAF cannot be improved any further, thus reaching a local optimum, or when the number of iterations exceeds a given large preset value. It should be mentioned that this procedure constitutes an improvement over the solution technique proposed in [18], since the proposed method updates the binary variable values based on the best local "direction" for SAF improvement as opposed to just using a somewhat random approach used in [18].

As discussed in [23], the method described in [18] can be considered a greedy heuristic approach, while the method proposed here is based on local search heuristics, which in general is considered more efficient. Notice that the proposed procedure yields a local feasible local optimum, which is all is needed in practice, considering the nature of the reactive power management problem and current ISO practices, which are rather heuristic and far from optimal in any particular sense. Observe as well that although global optimum search approaches such as evolutionary programming techniques (e.g. genetic algorithms) could be used to solve the proposed MINLP problem, the large computational costs associated with these methods would make them impractical [24]. Furthermore, it should be mentioned that the proposed heuristic technique is more efficient than other known MINLP solvers such as BARON and DICOPT, which fail to yield solutions for similar problems as shown in [18] and [24].

As per the aforementioned discussion, it is important to mention that the optimal solution generated by the proposed technique is dependent on the initial starting point, as discussed in [18]. Hence, to guarantee a reasonable solution, ISOs' current "best practice" approach is used to obtain the initial solution point. Accordingly, the initial values of Q_G are readily obtained from a power flow solution associated with the known values P_S, which come from the active power dispatch process; these are typically the reactive power dispatch levels used by most ISOs nowadays. This feasible point can be regarded as a reasonable starting point, particularly considering that it is available without any significant extra effort.

IV. Results and Comparisons

The CIGRE-32 and a 1211-bus dispatch model of a European network are used to study and compare the effect of different representations of reactive power limits in the maximum loading calculations, OPF-based market model and Q-procurement problem. The numerical studies were carried out in the AMPL environment using the interior point method solver IPOPT [25], [26]. To simplify the referencing to the various optimization models compared and discussed here, an identification tag for each model is adopted as per Table I. Observe that there is no R1 model, since no procurement models have been defined without the use of an opportunity region, as discussed in Section II.C.

A. Capability Curve Parameters

Before presenting the simulation results, a brief discussion on extracting from the standard power flow data the various parameters needed to represent the generator capability curves

TABLE I
MODEL TAGS

OPF Type	Q-limits Representation	Tag
Loadability Calc.	Simple Fixed	L1
	(3)	L2
	(7)	L3
Energy Auction	Simple Fixed	M1
	(3)	M2
	(9)	M3
Reactive Power Proc.	(3)	R2
	(10)	R3

is presented first, so that the data is consistent and the comparisons are meaningful. Thus, three generator parameters, X_S, $I_{a\max}$ and $E_{f\max}$, are required; however, the values of these parameters usually are not provided in typical power-flow data sets. Hence, these parameter values need to be determined from the available data, considering the generators' rated values.

A generator capability is the highest acceptable continuous loading in MVA (apparent power) under specified conditions of operation. For a generator operated at rated voltage, frequency and coolant conditions, its capability is equal to the output rating [27], [28]. Therefore, assuming that the cooling system and frequency are fixed at their rated values, the generated rated values are taken to be the values provided in the power flow data, which correspond to point M in Fig.2 [21]. Hence, the rated MVA of a specific machine is assumed to be given by:

$$S_{G_M} = \sqrt{P_{S_M}^2 + Q_{G_M}^2}. \tag{11}$$

where Q_{G_M} corresponds, as mentioned in Section II.D, to the maximum reactive power in the power flow data.

A typical value for the synchronous reactance of a generator, X_G, usually lies in the range 0.6 p.u. to 1.5 p.u., in the generator's own base. Hence, it is assumed here that $X_G = 1$ p.u., which allows to readily obtain the required values of X_S as follows:

$$X_S = \left(\frac{S_B}{S_{G_M}}\right)\left(\frac{V_G}{V_B}\right)^2. \tag{12}$$

where the subscripts B refers to the system base values, and V_G stands for the generator's base voltage, which is typically the same as V_B.

The maximum stator current of a generator is obtained by dividing its rated apparent power value S_{G_M} by its rated terminal voltage [27], [28]. Since, the value of V_{to} is typically provided as part of the generator's parameters in the power flow data, the value of $I_{a\max}$ in p.u. for a given generator may be calculated as follows:

$$I_{a\max} = \frac{S_{G_M}}{V_{to}}. \tag{13}$$

The generator's maximum excitation voltage $E_{f\max}$ may then be calculated as follows:

$$E_{f\max} = \frac{X_S}{V_{to}}\sqrt{\left(Q_{G_M} + \frac{V_{to}^2}{X_S}\right)^2 + P_{S_M}^2}. \tag{14}$$

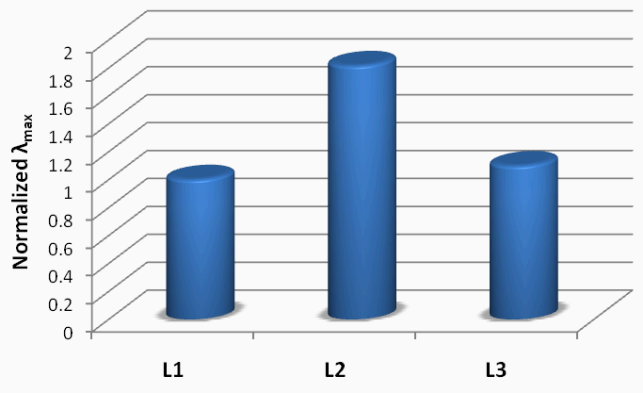

Fig. 6. Normalized maximum loadability values λ_{max} for different OPF models for the CIGRE-32 test system.

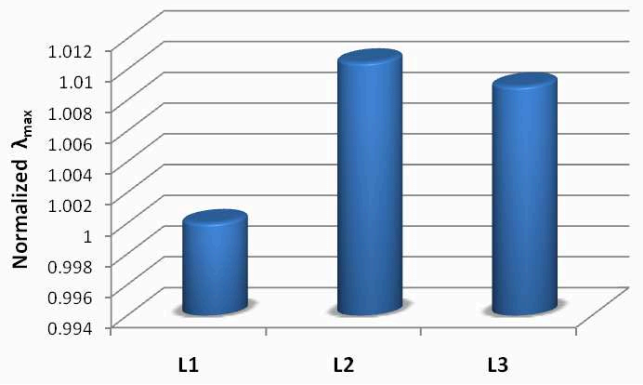

Fig. 7. Normalized maximum loadability values λ_{max} for different OPF models for the 1211-bus test system.

The generators' minimum reactive power limits provided in the power flow data set are used to define $Q_{G\min}$ in all models. Finally, to allow for more relevant results and comparisons, and without loss of generality, the value of $P_{S\max}$ (prime mover limits) are assumed here to be $1.1\ P_{S_M}$ and $1.04\ P_{S_M}$ for CIGRE-32 and 1211-bus test systems, respectively.

B. Maximum Loadability Studies

For the CIGRE-32 test system, the maximum loadability values $\lambda_{\max}$ for the three different models L1, L2 and L3 are depicted in Fig.6, normalized with respect to the value obtained for L1 for comparison purposes. For the 1211-bus system model, similar plots are shown in Fig.7. Observe in Fig.6 and Fig.7 that the L2 model presents the largest maximum loadability values, with the L3 model following. The reason for the L2 model yielding larger values than L3 is due to the fact that the Q-limits in L2 are higher than those associated with I_a limits in L3, as discussed in Section II.D, since the terminal voltage of every generator at the solution

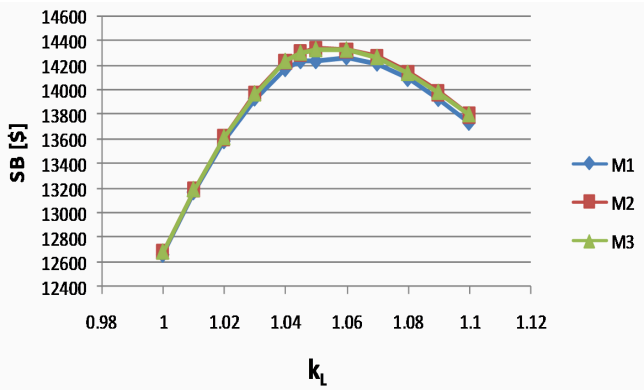

Fig. 8. Social benefit as load increases for the different generator reactive power limit models for the CIGRE-32 system.

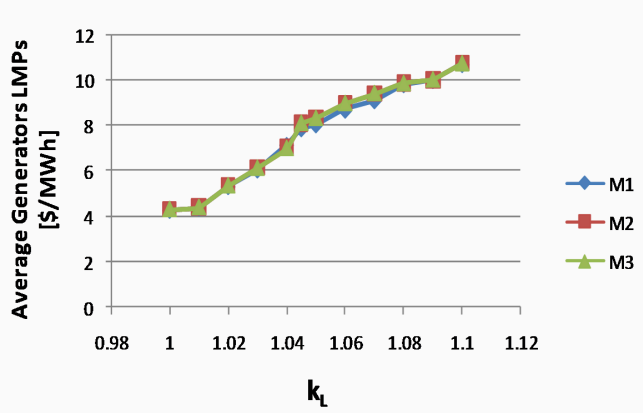

Fig. 9. Average supply-side LMPs for the different generator reactive power limit models for the CIGRE-32 system.

point for L3 is equal or smaller than V_{to}, whereas the L2 model limits are insensitive to generator voltage reductions; note in Fig.3 that the Q-limits associated with E_f remain practically unchanged as the terminal voltage changes. On the other hand, the L1 model yields the lowest values mainly because of the extra reactive power capability available in the L2 and L3 models associated with the representation of E_f limits, as explained in Section II.D (see Fig.2).

C. Market Auction Studies

1) CIGRE System: In this case the demand was assumed to be elastic, i.e. the demand is assumed to participate in the auction by providing power and price bids. To better compare the different models, different loading conditions were considered by gradually increasing the load levels by multiplying the demand maximum and minimum power bids $P_{D\min}$ and $P_{D\max}$ by a factor k_L.

The SB values and supply- and demand-side LMPs obtained for the 3 different market models M1, M2 and M3 as load levels increase are depicted in Fig.8, Fig.9 and Fig.10, respectively. Also, Fig.11 shows the average values of voltage magnitudes over all buses, and Fig.12 illustrates the active power losses in the grid. Observe that all models present very similar values in all cases. The reason for these similarities is the fact that, in the case of inelastic load, the load responsiveness to system conditions diminishes the effect of a better representation of the generator reactive power limits. This is confirmed by the results obtained for the European network, which is more realistically assumed to have an inelastic demand, resulting in more significant differences in voltage magnitudes and losses for the different modeling of generator reactive power limits, as discussed next.

2) 1211-Bus System: For this test system, the demand is assumed to be inelastic, which is the usual case in practice [10]. Accordingly, the objective of the problem turns into simply minimizing the electricity production costs; hence, the following classic quadratic cost function for generators

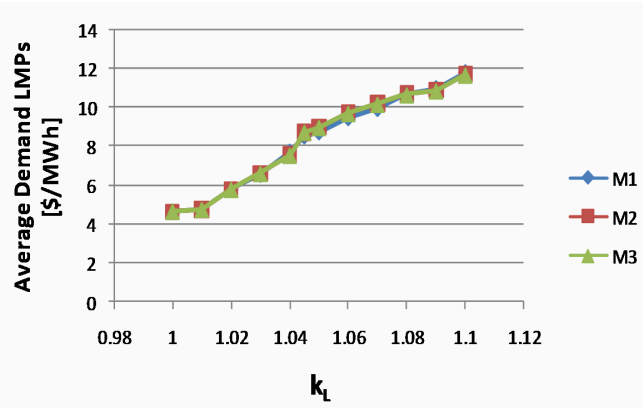

Fig. 10. Average demand-side LMPs for the different generator reactive power limit models for the CIGRE-32 system.

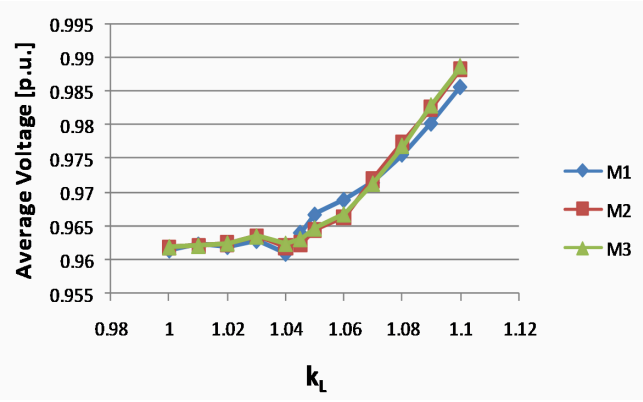

Fig. 11. Average voltage magnitudes for the different generator reactive power limit models for the CIGRE-32 system.

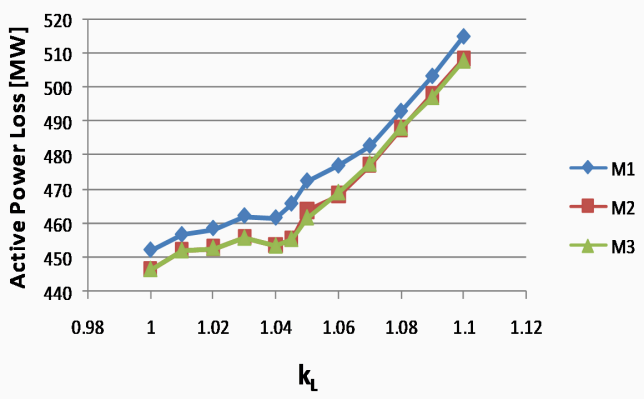

Fig. 12. Active power losses for the different generator reactive power limit models for the CIGRE-32 system.

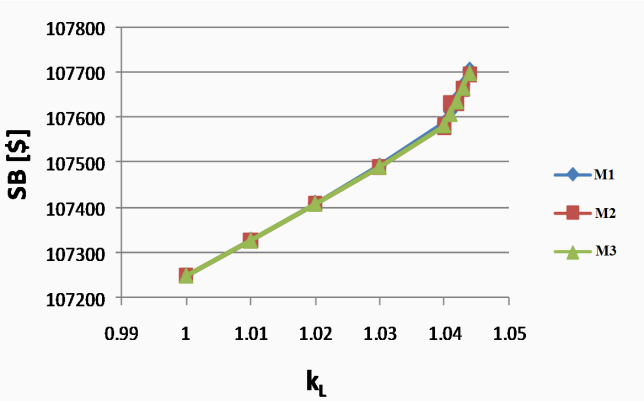

Fig. 13. Social benefit as load increases for the different generator reactive power limit models for the 1211-bus system.

is adopted here:

$$C\left(P_S\right) = \sum_{i \in \mathcal{G}} \left(a_i P_{S,i}^2 + b_i P_{S,i} + c_i\right) \tag{15}$$

where a_i, b_i and c_i are cost parameters of i^{th} generator, which were all available for this network.

The load levels were increased also using a multiplying factor k_L to examine and compare the models' performances. Figures 13 to 15 show the SB values and supply- and demand-side LMPs as k_L changes for the 3 different market models M1, M2 and M3; similarly to the Cigre-32 case, these results are very similar with no noticeable differences among all models. Figures 16 and 17, on the other hand, show more significant differences among the models for voltage magnitudes and power losses, with the model that has the most reactive power reserves (M2) yielding the best voltage profiles and lowest losses, and the model with the least reserves (M1) yielding exactly the opposite results, which is to be expected.

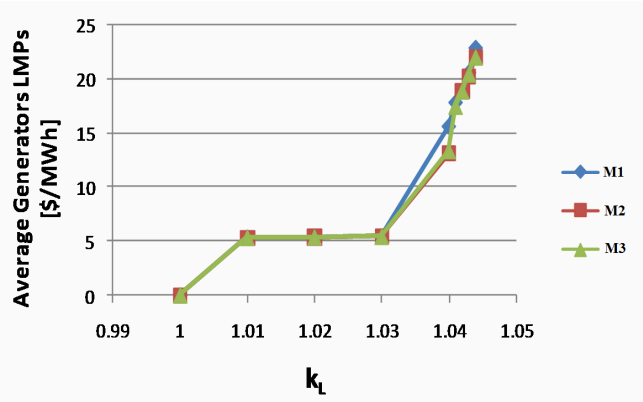

Fig. 14. Average supply-side LMPs for the different generator reactive power limit models for the 1211-bus system.

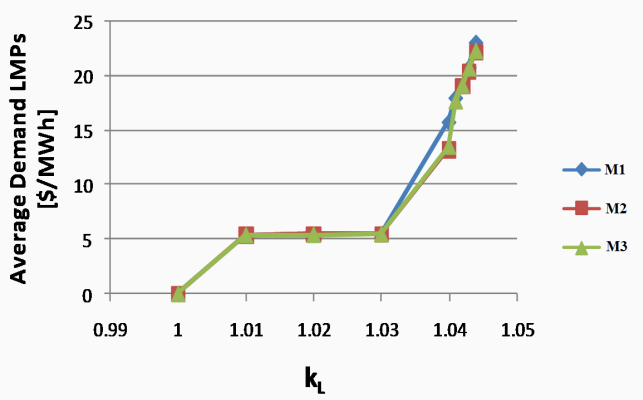

Fig. 15. Average demand-side LMPs for the different generator reactive power limit models for the 1211-bus system.

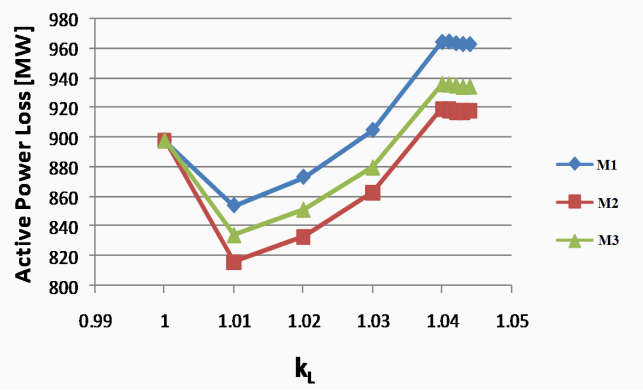

Fig. 16. Active power losses for different generator reactive power limit models for the 1211-bus system.

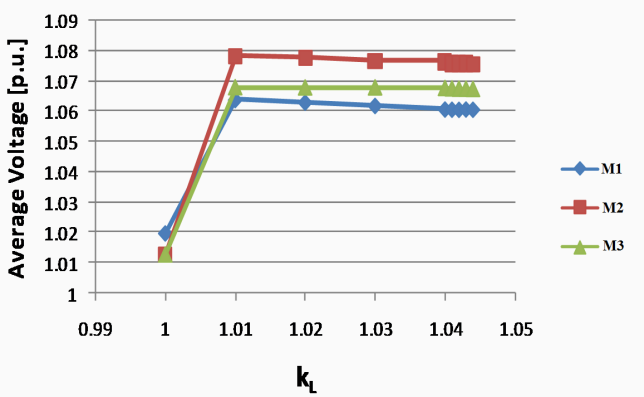

Fig. 17. Average voltage magnitudes for different generator reactive power limit models for the 1211-bus system.

TABLE II
CIGRE-32 SYSTEM Q-PROCUREMENT RESULTS

	R2	R3	% Change
SAF [$]	87958	87698.2	-0.30
ISO Pay [$]	1906.5	1927.11	+1.09
$\sum V$ [p.u.]	39.1941	39.1892	-0.01
$\sum Q_G$ [p.u.]	8.18	8.22	+0.49

D. Reactive Power Procurement Studies

In the following studies, C_L is assumed to be 100 $/MWh, which is a relatively typical high value for the Hourly Ontario Energy Price (HOEP) [29]. The generators are assume to be compensated over the whole capability region for losses, as it is done for example in Ontario [18]; thus, $Q_{G_{\text{lead}}}$ and $Q_{G_{\text{lag}}}$ are both set to zero.

1) CIGRE System: For the Cigre-32 system the values of Q_{G_A}, the m bids, and security sensitivity factors μ, η and γ are all assumed to be the same as in [18]. In this reference, the authors consider two loading conditions, namely, light and heavy loading; here, the latter case is used, since it corresponds to stressed system conditions, but with some minor generator and load dispatch level differences. The main results of applying the original R2 procurement model and the proposed R3 model are illustrated in Table II, where the values of SAF, expected Independent System Operator (ISO) payments, sum of voltage magnitudes over the grid and the sum of the values of generated reactive powers are presented. Observe that the SAF and voltage profiles are higher for R2 than R3, whereas the ISO payments for reactive power and total generated reactive powers are lower. This was expected from the previous comparisons presented in this section, since for the given stressed conditions, when the effect of generator terminal voltages in the corresponding capability curves are considered in model R3, generators at their capability limits in the voltage depleted regions generate less reactive power support with respect to model R2, forcing generators away from these regions to generate more reactive power to try to support these system voltages.

TABLE III
1211-BUS SYSTEM Q-PROCUREMENT RESULTS

	R2	R3	% Change
SAF	51895.4	69284.5	+33.78
ISO Pay [$]	25933.6	8815.05	-66.01
$\sum V$ [p.u.]	1285.52	1227.13	-4.54
$\sum Q_G$ [p.u.]	541.861	549.447	+1.4

TABLE IV
COMPUTATIONAL COSTS FOR THE 1211-BUS SYSTEM

	R2	R3
CPU Time [s]	14.11	1572.5
Iterations k in Fig.6	1	12

2) 1211-bus System: This system was divided into five "voltage" zones based on the system security sensitivity factors μ, η and γ, obtained from the OPF-DM calculations discussed in Section IV.B, since these values reflect the sensitivity of the system's maximum loadability with respect to reactive power injections at different buses. There are a total number of 190 generator buses, and the corresponding bidding values for reactive power, i.e. m_0, m_1, m_2 and m_3, were chosen based on the following criteria:

- For the availability value m_0, if the generator is dispatched for active power, this value was assumed to be zero, following Ontario's reactive power pricing policies [18]. On the other hand, if the generator is not generating active power, then this value is set to $m_0 = a$ in the cost equation (15).
- The prices $m_1 = m_2$ were chosen based on the active power loss prices that can be determined from the corresponding cost equation (15), and a linearization of the relation between reactive power and active power losses of each generator at point M in Fig.2.
- For m_3, a similar approach to the estimation of m_1 and m_2 was followed, but using in this case a linearization of the relation between reactive power and active power output of each generator at point M in Fig.2.

The values of SAF, expected ISO payments, sum of voltage magnitudes over the grid, and sum of the values of generated reactive powers are presented in Table III for both models R2 and R3. Note that the overall results voltages and reactive power are similar to the ones obtained for the 32-bus CIGRE system, i.e. voltages in general decrease while generator reactive powers increase in model R3 with respect to R2, for the same voltage support and Q-limit reasons explained in the previous section. However, the changes in SAF and ISO payments are the opposite and quite significant, which is mainly due to the significant differences in the assumed bids between the two test systems.

Finally, Table IV compares the computational burden between the R2 and R3 models in an IBM Windows sever with 8 32-bit processors. It is clear that the R2 model is more economical from the computational point of view, which is to be expected given the higher complexity of the R3 model.

V. Conclusions

A comparative assessment of different representations of reactive power limits in the context of 3 different OPF applications in voltage stability and electricity market studies, namely, maximum loadability calculations, an energy auction and a reactive power procurement procedure, was carried out. The accurate representation of generator capability limits in these OPF models, where field and armature current limits as well as terminal voltages are explicitly considered, was studied and discussed. The various OPF models were applied to the CIGRE 32-bus benchmark system and a 1211-bus model of a European grid, analyzing the effects that the different representation of Q-limits have on the associated results.

The different studies presented in this paper clearly show that the better representation of generator capability limits is important under stressed conditions, with the explicit representation of generator terminal voltages on generator capability limits playing a dominant role. However, in most cases, the observed differences may not be that significant to justify the increased computational complexity in practical applications.

References

[1] T. V. Cutsem and C. Vournas, *Voltage Stability of Electric Power Systems*. Boston: Kluwer, 1998.

[2] W. D. Rosehart, C. A. Cañizares, and V. H. Quintana, "Effect of detailed power system models in traditional and voltage-stability-constrained optimal power-flow problems," *IEEE Trans. Power Syst.*, vol. 18, no. 1, pp. 27–35, Feb. 2003.

[3] "Voltage stability assessment: Concepts, practices and tools," IEEE/PES Power System Stability Subcommittee, Tech. Rep. SP101PSS, Aug. 2002.

[4] V. Ajjarapu and C. Christy, "The continuation power flow: a tool for steady state voltage stability analysis," *IEEE Trans. Power Syst.*, vol. 7, no. 1, pp. 416–423, Feb. 1992.

[5] G. D. Irisarri, X. Wang, J. Tong, and S. Mokhtari, "Maximum loadability of power systems using interior point nonlinear optimization method," *IEEE Trans. Power Syst.*, vol. 12, no. 1, pp. 162–172, Feb. 1997.

[6] W. Rosehart, C. Roman, and A. Schellenberg, "Optimal power flow with complementarity constraints," *IEEE Trans. Power Syst.*, vol. 20, no. 2, pp. 813–822, May 2005.

[7] R. J. Avalos, C. A. Cañizares, F. Milano, and A. Conejo, "Equivalency of continuation and optimization methods to determine saddle-node and limit-induced bifurcations in power systems," *IEEE Trans. Circuits Syst. I*, vol. 56, no. 1, pp. 210–223, Jan. 2009.

[8] P. A. Löf, G. Andersson, and D. J. Hill, "Voltage dependent reactive power limits for voltage stability studies," *IEEE Trans. Power Syst.*, vol. 10, no. 1, pp. 220–228, Feb. 1995.

[9] J. A. Momoh *et al.*, "Challenges to optimal power flow," *IEEE Trans. Power Syst.*, vol. 12, no. 1, pp. 444–447, Feb. 1997.

[10] D. Kirschen and G. Strbac, *Fundamentals of Power System Economics*. Chichester: Wiley, 2004.

[11] M. Shahidehpour, H. Yamin, and Z. Li, *Market Operations in Electric Power Systems*. New York: Wiley, 2002.

[12] Z. S. Machado, G. N. Taranto, and D. M. Falcao, "An optimal power flow formulation including detailed modeling of generators," in *Proc. Power Systems Conference and Exposition (PSCE)*, Oct. 2004, pp. 960–965.

[13] F. Milano, C. A. Cañizares, and A. J. Conejo, "Sensitivity-based security-constrained OPF market clearing model," *IEEE Trans. Power Syst.*, vol. 20, no. 4, pp. 2051–2060, Nov. 2005.

[14] B. Tamimi and S. Vaez-Zadeh, "An optimal pricing scheme in electricity markets considering voltage security cost," *IEEE Trans. Power Syst.*, vol. 23, no. 2, pp. 451–459, May 2008.

[15] G. Chicco and G. Gross, "Current issues in reactive power management: A critical overview," in *Proc. IEEE Power and Energy Society General Meeting*, July 2008, pp. 1–6.

[16] S. Hao, "A reactive power management proposal for transmission operators," *IEEE Trans. Power Syst.*, vol. 18, no. 4, pp. 1374–1380, Nov. 2003.

[17] K. Bhattacharya and J. Zhong, "Reactive power as an ancillary service," *IEEE Trans. Power Syst.*, vol. 16, no. 2, pp. 294–300, May 2001.

[18] I. El-Samahy, K. Bhattacharya, C. Cañizares, M. F. Anjos, and J. Pan, "A procurement market model for reactive power services considering system security," *IEEE Trans. Power Syst.*, vol. 23, no. 1, pp. 137–149, Feb. 2008.

[19] M. J. Rider and V. L. Paucar, "Application of a nonlinear reactive power pricing model for competitive electric markets," *IEE Proc.-Gener. Transm. Distrib.*, vol. 151, no. 3, pp. 407–414, May 2004.

[20] M. A. Tabrizi and M. E. H. Golshan, "Comprehensive model for simultaneous pricing of active and reactive power based on marginal cost theory," in *Proc. IEEE PECon 08*, Malaysia, Dec. 2008, pp. 1–6.

[21] C. W. Taylor, *Power System Voltage Stability*. New York: McGraw-Hill, 1994.

[22] Y. Kataoka and Y. Shinoda, "Voltage stability limit of electric power systems with generator reactive power constraints considered," *IEEE Trans. Power Syst.*, vol. 20, no. 2, pp. 951–962, May 2005.

[23] J. P. Walser, *Integer Optimization by Local Search*. Singapore: Springer, 1999.

[24] M. B. Liu, C. A. Cañizares, and W. Huang, "Reactive power and voltage control in distribution systems with limited switching operations," *IEEE Trans. Power Syst.*, vol. 24, no. 2, pp. 889–899, May 2009.

[25] R. Fourer, D. Gay, and B. Kernighan, *AMPL: A Modeling Language for Mathematical Programming*. Pacific Grove, CA: McGraw-Hill, 2003.

[26] A. Wächter and L. T. Biegler, "On the implementation of a primal-dual interior point filter line search algorithm for large-scale nonlinear programming," *Mathematical Programming*, vol. 106, no. 1, pp. 25–57, 2006.

[27] *Cylindrical-Rotor 50 Hz and 60 Hz Synchronous Generators Rated 10 MVA and Above*, IEEE Std. C50.13-2005, Feb. 2006.

[28] *Salient-Pole 50 Hz and 60 Hz Synchronous Generators and Generators/Motors for Hydraulic Turbine Applications Rated 5 MVA and Above*, IEEE Std. C50.12-2005, Feb. 2006.

[29] The IESO website. [Online]. Available: http://www.ieso.ca

Behnam Tamimi (S'05) received the B.Sc. degree in Electronics Eng. from the University of Tehran, Tehran, Iran in 2001 and the M.Sc. degree in Electrical Eng. from KNT University, Tehran, Iran, in 2003. He is currently a Visiting Scholar at the University of Waterloo, and is pursuing the Ph.D. degree at University of Tehran. His research interests include power system analysis and control and power electronics applications in power systems.

Claudio A. Cañizares (S'85, M'91, SM'00, F'07) received the Electrical Engineer degree from Escuela Politécnica Nacional (EPN), Quito-Ecuador, in 1984 where he held different teaching and administrative positions from 1983 to 1993. His MSc (1988) and PhD (1991) degrees in Electrical Engineering are from University of Wisconsin-Madison. He has been with the E&CE Department, University of Waterloo since 1993, where he has held various academic and administrative positions and is currently a full Professor and the Associate Director of the Waterloo Institute for Sustainable Energy (WISE). His research activities concentrate in the study of stability, modeling, simulation, control and computational issues in power systems within the context of competitive electricity markets.

Dr. Cañizares has been the recipient of various IEEE-PES Working Group awards, and currently holds and has held several leadership appointments in IEEE-PES technical committees and subcommittees, as well as working groups and task forces.

Sadegh Vaez-Zadeh Sadegh Vaez-Zadeh (S'95, M'03, SM05) received the B.Sc. degree from Iran University of Science and Technology, Tehran, Iran in 1985 and the M.Sc. and Ph.D. degrees from Queen's University, Kingston, ON, Canada, in 1993 and 1997 respectively, all in Electrical Engineering. He has been with several research and educational institutions in different positions before joining the University of Tehran as an Assistant Professor in 1997 where he became an Associate Professor in 2001 and a Full Professor in 2005. He served the university as the Head of Power Division from 1998 to 2000 and currently is the Director of Advanced Motion Systems Research Laboratory which he founded in 1998 and the Director of Electrical Engineering Laboratory since 1998. His research interests include advanced rotary and linear electric machines and drives, magnetic levitation, electric vehicles and power system analysis and control. He has published about 150 research papers in these areas. He is an Editor of IEEE Transactions on Energy Conversion, and a co-founder and a member of the editorial board of Iranian Journal of Electrical and Computer Engineering. He is also a member of editorial board of the Journal of Faculty of Engineering as the oldest engineering journal in the Middle East. He has served many IEEE sponsored conferences as a member of technical and steering committees, session chair, etc.

Prof. Vaez-Zadeh is a member of IEEE PES Motor Sub-Committee and Power System Stability Control Sub-Committee. He has received a number of awards domestically including a best paper award from Iran Ministry of Science, Research and Technology in 2001 and a best research award from the University of Tehran in 2004.